



## ADSORPTION OF THE ANTIBIOTIC ROXITHROMYCIN ON LOW-COST FOOD WASTE MATERIALS: BATCH AND COLUMN STUDIES

İlknur TOSUN SATIR<sup>1</sup>, Bediha AKMEŞE<sup>2\*</sup>

<sup>1</sup>Hitit University, Faculty of Arts and Sciences, Department of Chemistry, 19040, Çorum, Türkiye

<sup>2</sup>Hitit University, Faculty of Vocational School of Health Services, Department of Pharmacy Services, 19030, Çorum, Türkiye

**Abstract:** Antibiotics are widely utilized for a variety of medical conditions. Antibiotic residues in wastewater are dangerous to all living beings. Antibiotics remain in the wastewater environment when general treatment plant technologies are employed. The literature has numerous techniques for getting rid of antibiotics. Compared to other techniques for removing contaminants in the solution environment, the adsorption method is preferred due to its benefits, such as ease of use, high efficiency, and low cost. The study investigated using the green walnut shell (GWS), a natural sorbent, as an adsorbent to discharge roxithromycin (ROX) antibiotics from the solution medium. Adsorption conditions were studied in batch and continuous systems. pH, adsorbent amount, interaction time, sorbate concentration, and salt effect parameters were investigated in the batch system. The data obtained were calculated with kinetic and isotherm models. The adsorption process has been based on the so-called pseudo-second-order kinetic model. GWS was characterized using SEM and FTIR techniques. The amount of adsorbent, flow rate, and breakdown in the continuous system were explored. In the batch system, the adsorption equilibrium was set up at the solution's original pH with 0.1 g of adsorbent in 40 minutes, and 79% ROX removal was achieved. The optimum flow rate and adsorbent amount in the continuous system were determined as 0.1 mL/min and 0.3 g, respectively.

**Keywords:** Wastewater, Adsorption, Roxithromycin, Green walnut shell, Removal, Antibiotic

\*Corresponding author: Hitit University, Faculty of Vocational School of Health Services, Department of Pharmacy Services, 19030, Çorum, Türkiye

E mail: bedihaakmese@hitit.edu.tr (B. AKMEŞE)

İlknur TOSUN SATIR  <https://orcid.org/0000-0003-3769-8767>

Bediha AKMEŞE  <https://orcid.org/0000-0002-6652-4574>

Received: March 29, 2024

Accepted: May 03, 2024

Published: May 15, 2024

Cite as: Tosun Satır İ, Akmeşe B. 2024. Adsorption of the antibiotic roxithromycin on low-cost food waste materials: batch and column studies. BSJ Eng Sci, 7(3): 521-528.

### 1. Introduction

Antimicrobial treatment studies started in the late 19th century. Since the first day of its production, antibiotics have attracted a lot of attention all over the World (Li et al., 2019). Antibiotics are widely used in a wide variety of treatment modalities in humans and animals. Antibiotics are excreted through the feces and urine; 50-80% of them are not metabolized after being taken into the body (Yang et al., 2016). Therefore, antibiotics pollute the environment by mixing into municipal wastewaters in unchanged form or using animal fertilizers as fertilizers. Contamination of wastewater with antibiotics poses a problem and poses a significant risk for all living things (Bai et al., 2015; Yin et al., 2016).

Recently, increased medication and especially antibiotic consumption has been a concern for both environmental protection and human health (Sharma et al., 2019). Since antibiotics cannot be removed with conventional aerobic sludge systems, the treatment plant is located in the outlet waters and receiving environments. Therefore, permanent concentrations of therapeutic antibiotics exist in the environment. High antibiotic concentration in the ecosystem creates toxicity for organisms and disrupts ecological balance (Topal et al., 2013).

Antibiotics contained in waste from animals or humans can be mixed into the environment through municipal wastewater treatment or land irrigation with recycled water. Similarly, animal and poultry manure may contain antibiotics that remain mostly unchanged. Antibiotics in these fertilizers have the potential to switch to the adjacent surfaces of the application point and application point to agricultural lands or to shallow groundwater (Topp et al., 2016). In these ways, antibiotics can reach the surface and groundwater (Rivera-Utrilla et al., 2013). Macrolide group antibiotics are broad-spectrum synthetic antibiotics that are widely used in medicine to treat humans and animals. Macrolide antibiotics have low water solubility. These reasons are found in low concentrations in the aqueous solution medium (Yang and Carlson, 2004). Roxithromycin (ROX), one of the macrolide antibiotics, is widely used in treatments and is produced in large quantities. It also has a long half-life. Considering all these reasons, their concentration in wastewater sources is significant, and treatment should be provided (Liu, 2018).

Various methods such as chemical precipitation, ultrafiltration, reverse osmosis, ion exchange, adsorption, solvent extraction and biological processes are applied to





injection volume was determined as 20 µL.

### 2.5. Adsorption Experiments

Adsorption conditions in batch and column systems were studied. In the batch system, 10 mL antibiotic solutions and GWS adsorbents were mixed with Bio RS-24 model rotator in the falcon tube. The pH of the ROX solutions was adapted with 0.1 M NaOH and 0.1 M HCl solutions. The kinetic studies were performed using 6 mg/L ROX solution at 25 °C. To determine the batch system conditions in the adsorption of GWS and ROX the effects of pH adsorbent amount, interruption time, adsorbate concentration ad, salt effect. In the continuous (column) system, flow rate, adsorbent amount, and breaking point were determined. Continuous system adsorption studies were prepared by filling GWS between two glass cotton in 5 mL injectors. The amount of biosorbent filled in the column was 0.30 g. The solution flow direction was adjusted from bottom to top. ROX solutions at a concentration of 6 mg/L and a volume of 10 mL were passed through the column at the adjusted flow rate through the prepared column system. ROX solutions were passed through the column designed with the flow direction upwards with a peristaltic pump (Akar et al, 2009).

The adsorption performance (q) of the adsorbent is expressed as the amount of antibiotic adsorbed (mg) per unit mass (g) of the GWS. q is calculated with Equation1.

$$q = \frac{C_0 - C_e}{m} \times V \quad (1)$$

here, q= adsorption capacity (mg/g), C<sub>0</sub>= concentration of antibiotic ion (mg/L), C<sub>e</sub>= concentration of antibiotic ions remaining in the equilibrium solution (mg/L), m= adsorbent dose (m), and V= solution volume (L).

## 3. Results and Discussion

### 3.1. Characterization of GWS

FT-IR spectra of the GWS before and after adsorption were taken to determine the functional groups of GWS. Figure 2 and Figure 3 show the spectra of GWS before and after adsorption, respectively. It belongs to the peak O-H stretch vibration observed at 3335 cm<sup>-1</sup> in both spectra. The peak at 2916 cm<sup>-1</sup> and 2850 cm<sup>-1</sup> is for the aliphatic C-H stretching, which shows that CH<sub>2</sub> and or CH<sub>3</sub> group may involve in ROX adsorption as peak shifts to 2920 cm<sup>-1</sup>. In addition, the increase in peak intensity at 2850 cm<sup>-1</sup> may indicate the presence of adsorption. The peak at 1236 cm<sup>-1</sup> is for C-O stretching, which suggests the ester group's presence and shifts to 1234 cm<sup>-1</sup> after adsorption. A sharp peak at 1027 cm<sup>-1</sup>, showing the glycosidic link between cellulose and glucose, belongs to the glycosidic C-H deformation with ring vibration and OH bending (Banerjee et al, 2018).

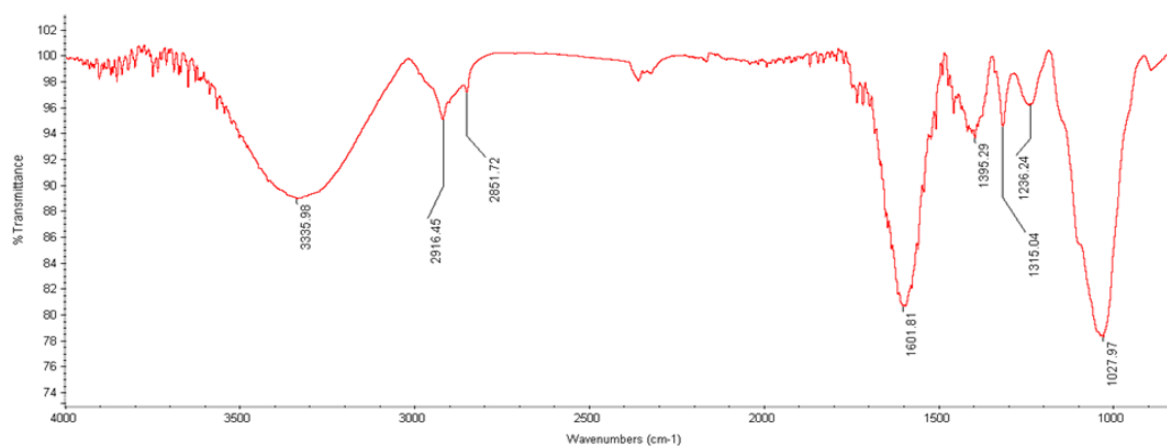


Figure 2. FTIR spectrum of GWS before adsorption.

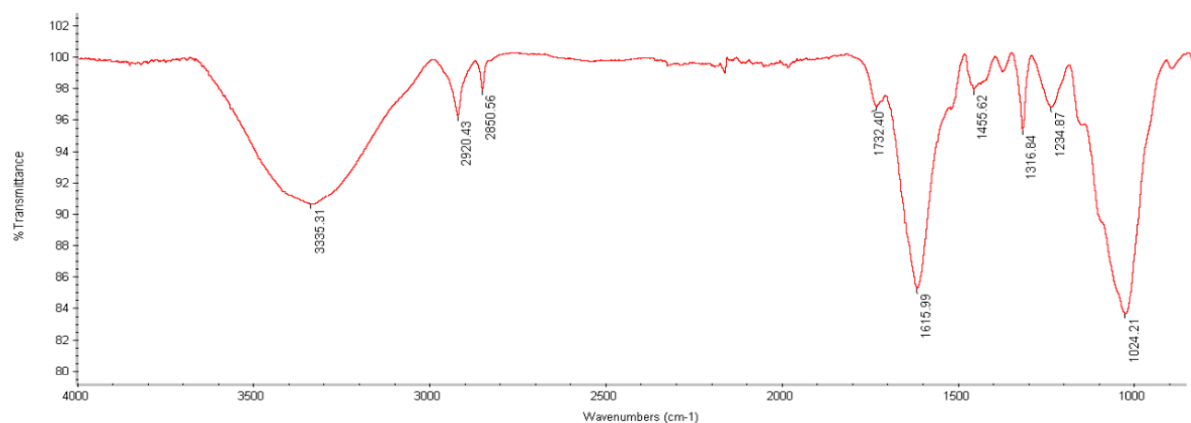
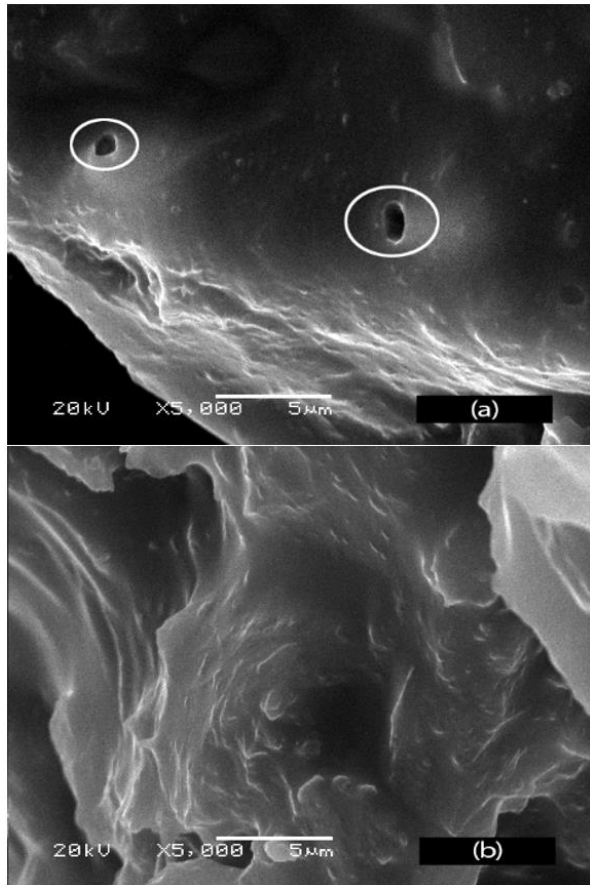


Figure 3. FTIR spectrum of GWS after adsorption.

The surface morphology of GWS (Figure 4 a and b) was detected using SEM techniques. When the figures were examined, it was seen that there were rough and porous areas on the surface of KWH to which ROX molecules could bind. After ROX adsorption on GWS, it was seen that the binding sites were coated with ROX molecules. The surface area (BET multipoint surface area - m<sup>2</sup>/g) of the GWS is 10.82 m<sup>2</sup>/g.



**Figure 4.** SEM pictogram of GWS a) before adsorption (scale bar-5 μm, X 5.000) b) after adsorption (scale bar-5 μm, X 5.000).

### 3.2. Batch System Studies

The effect of the pH of the ROX was analyzed. pH-dependent variation of the adsorption efficiency was investigated in the range of pH 2.5-3.5. The pH-dependent change of the adsorption efficiency for the ROX discharge by GWS was given in Figure 5. The figure shows that the adsorption capacity increased to pH 5.5, but there was no significant change at higher pH values.

The dose of GWS was explored at the optimum pH and in the range 0.02-0.20 g (Figure 6). As the amount of GWS increased, the adsorption efficiency increased. The adsorption efficiency remained constant after 0.1 g of the adsorbent amount. The optimum adsorbent amount was determined as 0.1 g.

Interaction time is an important parameter that should be examined in adsorption studies. Therefore, it was studied at a time interval of 5-90 minutes and at room temperature. As seen in Figure 7, the adsorption

efficiency increased until 40 minutes, and no change was seen after this time point. The equilibrium time was determined as 40 minutes, and subsequent studies continued using this time point.

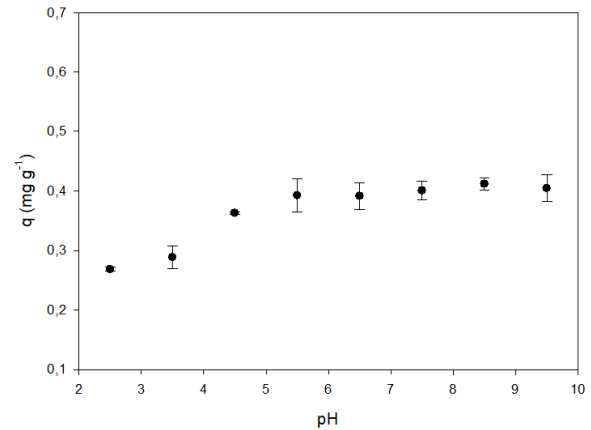


**Figure 5.** Effect of initial pH.

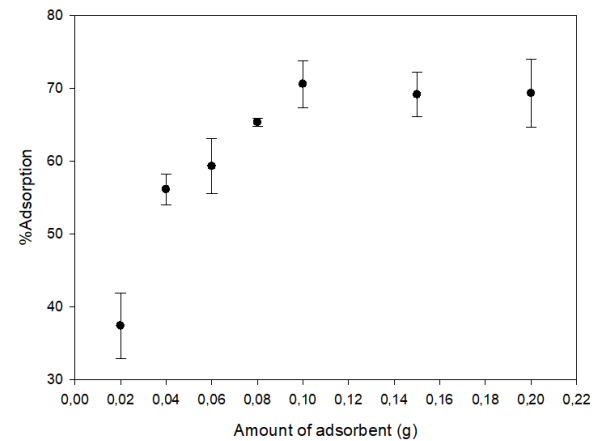


**Figure 6.** Effect of adsorbent dose.

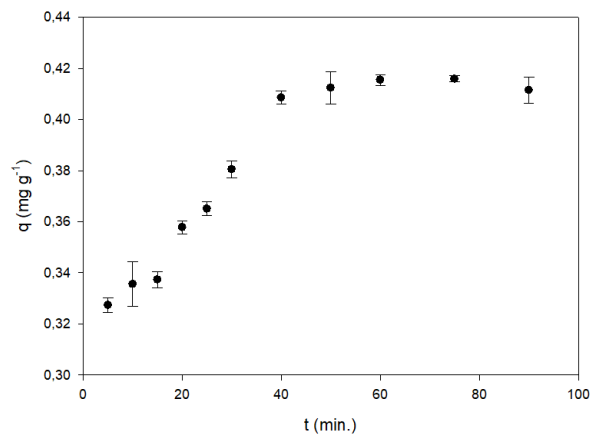


**Figure 7.** Effect of interaction time.

The effect of ionic strength (salt effect) on distillation water by GWS was realized in the batch system under optimum operating conditions determined by previous studies. For this purpose, NaCl was added to the medium at concentrations ranging from 0.01-0.15 M. ROX removal decreased from 79.79% to 54.80% when the NaCl concentration in the environment was increased from 0.01 to 0.1 M (Figure 8). According to these data, it is

seen that ionic strength slightly decreases the adsorption performance of GWS. Based on these data, it can be said that the ion exchange mechanism may be slightly effective in the adsorption of ROX dye to the GWS surface. In other words, the ionic strength in the concentration range studied did not dramatically affect the adsorption performance of ROX. Considering the high salt content of actual wastewater environments, this is an advantage.

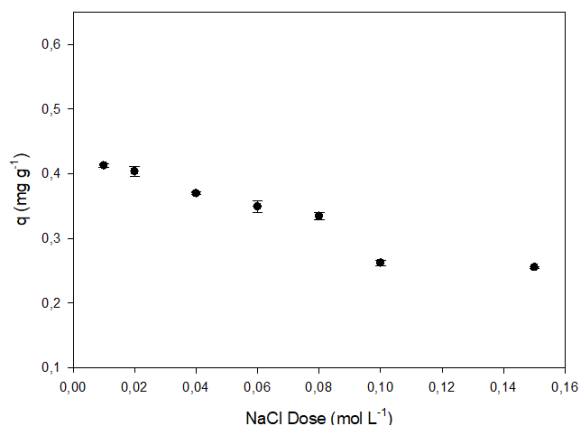


Figure 8. Salt effect.

### 3.3. Kinetic Parameters

Experimental data obtained from the interaction time study were evaluated using 3 kinetic models. The equation was first assessed with the first-order kinetic model equation (Equation 2) (Lagergren, 1898).

$$\ln(q_e - q_t) = \ln q_e - k_1 t \quad (2)$$

here;  $q_e$ = amount of substance adsorbed in equilibrium ( $\text{mg g}^{-1}$ ),  $q_t$ = adsorption capacity at time  $t$  ( $\text{mg/g}$ ),  $t$ = time (min.),  $k_1$ = pseudo-first-order rate constant ( $1/\text{min}$ ).

The data obtained from the experimental study were applied to the so-called first-order kinetic model, and the results were presented in Table 1. The value of  $r^2$  was found to be 0.780. It was seen that the change in this result was not linear. Also, it was determined that the  $q_e$  values calculated using the cut-off points were not within acceptable limits. These data showed that the adsorption process did not occur with a so-called first-order reaction.

Table 1. Kinetic parameters

Pseudo-first-order		Pseudo-second-order		Intraparticle diffusion	
$q_e$ ( $\text{mg g}^{-1}$ )	0.205	$q_e$ ( $\text{mg g}^{-1}$ )	0.423	$C$ ( $\text{mg g}^{-1}$ )	0.295
$k_1$ ( $\text{min}^{-1}$ )	$7.9 \times 10^{-2}$	$k_2$ ( $\text{g mg}^{-1} \text{min}^{-1}$ )	0.346	$K_p$ ( $\text{mg g}^{-1} \cdot \text{min}^{-1/2}$ )	$1.44 \times 10^{-2}$
$r^2$	0.780	$r^2$	0.991	$r^2$	0.881

Table 2. Isotherm parameters

Langmuir		Freundlich		D-R	
$q_{\max}$ ( $\text{mol g}^{-1}$ )	$9.206 \times 10^{-7}$	$n$	3.23	$q_{\max}$ ( $\text{mol g}^{-1}$ )	$3.786 \times 10^{-6}$
$q_{\max}$ ( $\text{mg g}^{-1}$ )	0.443	$K_F$ ( $\text{L g}^{-1}$ )	$2.247 \times 10^{-5}$	$\beta$ ( $\text{mol}^2 \text{kJ}^{-2}$ )	$2.65 \times 10^{-9}$
$K_L$ ( $\text{L mol}^{-1}$ )	$3.62 \times 10^5$	$r^2$	0.768	$E$ ( $\text{kJ mol}^{-1}$ )	$1.337 \times 10^4$
$r^2$	0.987			$r^2$	0.810

The pseudo-second-order kinetic model equation (Ho and McKay, 1999) is expressed by Equation 3.

$$\frac{1}{q_t} = \frac{1}{k_2 q_e^2} + \frac{1}{q_e} t \quad (3)$$

here;  $q_e$ = amount of substance adsorbed in equilibrium ( $\text{mg g}^{-1}$ ),  $q_t$ = adsorption capacity at time  $t$  ( $\text{mg/g}$ ),  $t$ = time (min.),  $k_2$ = pseudo-second-order rate constant ( $\text{g/mg min}$ ).

In the graph of  $t$  vs  $t / q_t$ , according to Equation 3, the slope is  $1 / q_e$ , and the ordinate axis cut-off point is  $1/k_2 q_e^2$ . The pseudo-second-order kinetic model plot is given in Fig.9. When the data in Figure 9 and Table 2 ( $r^2 = 0.991$ ) were examined, linearity was observed. Also, the  $q_e$  value calculated from the kinetic model was in agreement with the experimental data.

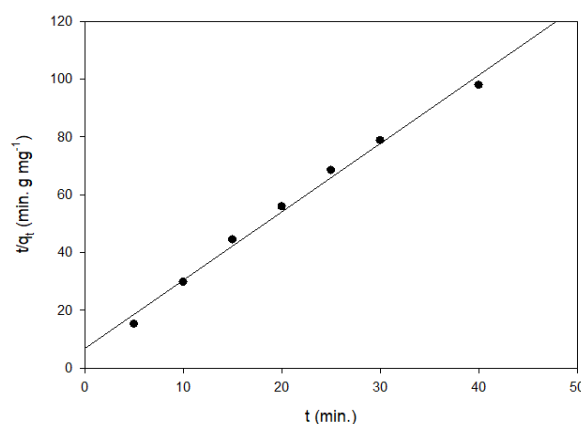


Figure 9. Pseudo-second-order model graphics.

The intraparticle diffusion model proposed by Weber and Morris (Weber and Morris, 1963) is expressed by Equation 4. The  $r^2$  value of the intraparticle diffusion model was calculated as 0.881. When all results were evaluated, it was seen that chemical adsorption was effective.

$$q_t = k_p t^{1/2} + C \quad (4)$$

here;  $q_t$ = adsorption capacity at time  $t$  ( $\text{mg/g}$ ),  $t$ = time (min.),  $k_p$ = Intraparticuler diffusion rate constant ( $\text{mg/g min}$ ), and  $C$ = constant value.

### 3.4. Isotherm Parameters

The equation showing the relation of the amount of a substance bound to the adsorbent surface at a constant temperature with its concentration in solution is called the adsorption isotherm. In this study, the initial adsorbate concentration experiment data were investigated with 3 different isotherm models.

The Langmuir adsorption isotherm refers to single-layer homogeneous adsorption. Each molecule has a fixed enthalpy and absorption energy. Langmuir adsorption isotherm is given in Equation 5 (Langmuir, 1916).

$$\frac{1}{q_e} = \frac{1}{q_{max}} + \left(\frac{1}{q_{max} K_L}\right) \frac{1}{C_e} \quad (5)$$

Figure 10 shows the Langmuir isotherm plot of the ROX molecule adsorbed on the GWS adsorbent. When the isotherm data given in Table 2 were examined, the  $r^2$  value of this isotherm was 0,987. Also, the theoretically calculated  $q_{max}$  value was  $0.443 \text{ mg g}^{-1}$ , and it was similar to the experimentally obtained  $q$  value. When all results were evaluated, it was seen that the adsorption data fit the Langmuir isotherm model.

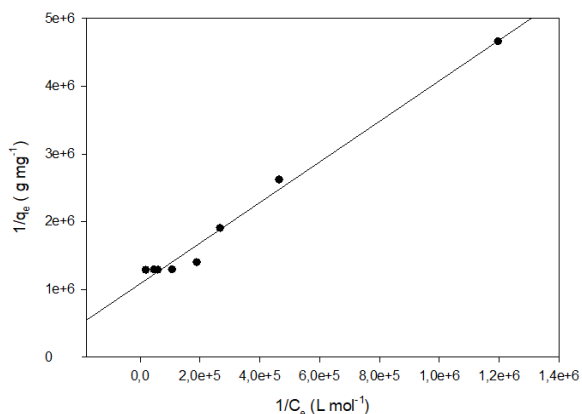


Figure 10. Langmuir isotherm model graphics.

Freundlich isotherm model explains multi-layer, irregularly distributed adsorption on a heterogeneous surface (Freundlich, 1906). The adsorbed amount is the sum of the adsorption in all regions, and when the adsorption is completed, the adsorption energy decreases exponentially (Roginsky and Zeldovich, 1934). This isotherm model is expressed by Equation 6.

$$\ln q_e = \ln K_F + \frac{1}{n} \ln C_e \quad (6)$$

The D-R adsorption isotherm is an isotherm model developed by Dubinin (Misra, 1969) for the interpretation of the adsorption equilibrium of organic compounds in the gas phase in mostly porous solids. However, it has also been applied for adsorption from the solution phase in many studies. In this isotherm model, it gives information about the binding pattern for the adsorption mechanism.

Isotherm was given in Equation 7:

$$\ln q_e = \ln q_m - \beta \varepsilon^2 \quad (7)$$

here:  $q_e$ = Amount of substance adsorbed on unit adsorbent at equilibrium (mol/g),  $q_{max}$ = Maximum adsorption capacity (mol/g),  $C_e$ = The molarity of the substance remaining in solution at equilibrium (mol/L),  $K_L$ = Langmuir isotherm constant (L/mol),  $K_F$ = Freundlich isotherm constant (L/g),  $n$ = Freundlich isotherm constant (unitless),  $\varepsilon$ = Polanyi potential, and  $\beta$ = Constant related to the mean free energy of adsorption per 1 mole of adsorbate ( $\text{mol}^2/\text{J}^2$ ).

The  $r^2$  values of Freundlich and D-R isotherm equations (Table 2) were calculated as 0.768 and 0.810, respectively. The order of suitability for the isotherm models was obtained in Langmuir/ D-R / Freundlich. It was seen from these data that ROX adsorption on GWS was realized in a single layer.

### 3.5. Column Adsorption Studies

Continuous system adsorption studies were carried out with GWS filled between two glass cotton in 2.5 ml injectors. The solution inlet was adjusted to the bottom of the column and was studied with ROX solution at a volume of 10 mL and a concentration of 6 mg/L.

The sorbate solution's flow rate is a necessary parameter affecting the adsorption performance in continuous system adsorption studies. For this purpose, 5 different flow rates were investigated. It was observed that the adsorption capacity decreased at speeds higher than 0.50 mg/min (Figure 11). The optimum flow rate was determined to be 0.5 ml min.

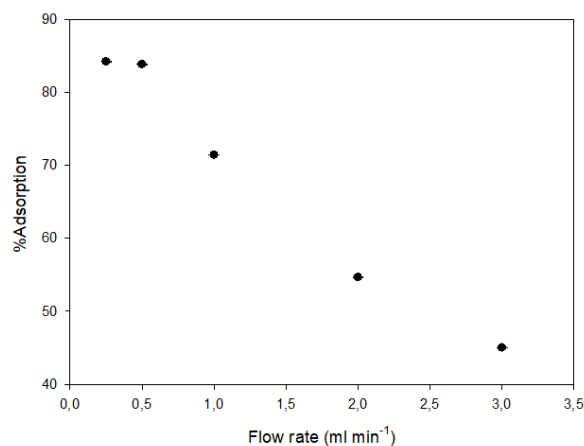


Figure 11. Effect of flow rate in a column system.

The amount of adsorbent filled in the column was changed in the range of 0.025-0.4 g, and ROX adsorption was investigated in the continuous system. The study was carried out with 6 mg/L ROX solutions at a 0.5 mL/min flow rate. The data obtained were given in Figure 12. As the GWS amount increased, the bed height of the column increased, so the contact time with the ROX solution increased, and thus the adsorption efficiency increased. The adsorption yield is fixed after 0.30 g.

A breakthrough was determined in the continuous system. Continuous monitoring of the output ROX ion concentration is given in Figure 13. In this figure, a characteristic S shape curve was observed, which is

favourable for continuous mode sorption applications. The breakthrough was determined around 20 minutes, and almost 87% of the ROX has been removed by this point. These results revealed that ROX adsorption with GWS could be a potential alternative for continuous system processing applications.

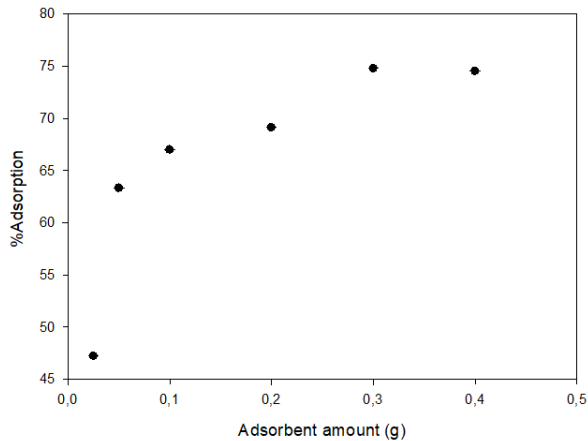


Figure 12. Effect of adsorbent dose in a column system.

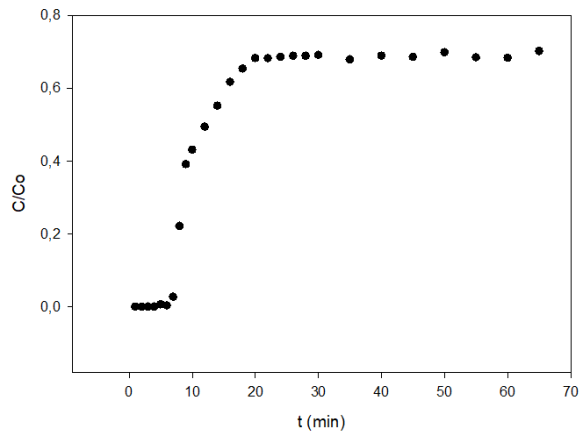


Figure 13. Breakthrough curve for ROX onto GWS.

#### 4. Conclusion

In this study, the removal of green walnut shells, a natural adsorbent, and roxithromycin, one of the macrolide group antibiotics, by adsorption method was investigated. For this purpose, in the batch system, starting solution pH, amount of adsorbent, temperature, time, initial antibiotic concentration, ionic strength; solution flow rate, adsorbent amount, and breakthrough parameters in the column system was examined. It was observed that when the pH of the ROX solution changed in the range of 5.5-9.5, it did not cause a significant change in the adsorption efficiency. According to these results, the optimum pH was determined as the original pH (pH 6.26) of the ROX solution. It is very advantageous not to adjust the pH in the removal of antibiotics from the wastewater environment by the adsorption method. In the batch system, the adsorption equilibrium was established in the amount of 0.1 g adsorbent and in a short time, like 40 minutes. Maximum adsorption efficiency was obtained in the column system at a flow

rate of 0.5 mL/min and an amount of 0.3 g adsorbent. In the batch system optimum conditions, 79% removal was achieved, and 87% removal was completed in the column system.

ROX adsorption by GWS was studied with pseudo-first-order, pseudo-second-order, and intraparticle diffusion models, and the data were found to fit the pseudo-second-order kinetic model. Also, adsorption data were examined with the Langmuir, Freundlich, and D-R isotherm models, and the most suitable model was determined as the Langmuir isotherm model. As a result, the green walnut shell, which is abundant in our country, has a natural adsorbent potential that is highly effective, highly efficient, economical, and easily obtainable for ROX removal from the wastewater environment.

#### Author Contributions

The percentage of the author(s) contributions is presented below. All authors reviewed and approved the final version of the manuscript.

	İ.T.S.	B.A.
C	50	50
D	60	40
S	50	50
DCP	50	50
DAI	50	50
L	40	60
W	60	40
CR	50	50
SR	40	60

C=Concept, D= design, S= supervision, DCP= data collection and/or processing, DAI= data analysis and/or interpretation, L= literature search, W= writing, CR= critical review, SR= submission and revision.

#### Conflict of Interest

The authors declared that there is no conflict of interest.

#### Ethical Consideration

Ethics committee approval was not required for this study because of there was no study on animals or humans.

#### References

- Akar ST, Gorgulu A, Anilan B, Kaynak Z, Akar T. 2009. Investigation of the biosorption characteristics of lead (II) ions onto *Symphoricarpos albus*: batch and dynamic flow studies. *J Hazard Mater*, 165(1-3): 126-133.
- Bai X, Ma X, Xu F, Li J, Zhang H, Xiao X. 2015. The drinking water treatment process as a potential source of affecting the bacterial antibiotic resistance. *Sci Total Environ*, 533: 24-31.
- Banerjee M, Basu RK, Das SK. 2018. Cr (VI) adsorption by a green adsorbent walnut shell: Adsorption studies, regeneration studies, scale-up design and economic feasibility. *Process Saf Environ Prot*, 116: 693-702.
- Freundlich H. 1906. Freundlich's Adsorption Isotherm. *Phys Chem*, 57: 384.
- Ho YSI, McKay G. 1999. Pseudo-second order model for sorption processes. *Process Biochem*, 34(5): 451-465.

- Huang Y, Wang Y, Huang Y, Zhang L, Ye F, Wang J, Shang J, Liao Q. 2020. Impact of sediment characteristics on adsorption behavior of typical antibiotics in Lake Taihu, China. *Sci Total Environ*, 718: 137329.
- Lagergren S, Lagergren S, Lagergren SY, Sven K. 1898. Zurtheorie der sogenannten adsorption gelösterstoffe. *Zeitschr f Chem und Ind der Kolloide*, 2: 15.
- Langmuir I. 1916. The constitution and fundamental properties of solids and liquids. Part I. Solids. *J Am Chem Soc*, 38(11): 2221-2295.
- Li Z, Li M, Zheng T, Li Y, Liu X. 2019. Removal of tylosin and copper from aqueous solution by biochar stabilized nano-hydroxyapatite. *Chemosphere*, 235: 136-142.
- Liu Z. 2018. Adsorption performance of roxithromycin on multi-walled carbon nanotubes in water. 7th International Conference on Energy and Environmental Protection, July 14-15, Shenzhen, China, pp: 880-886.
- Mahmoud DK, Salleh MAM, Karim WAWA, Idris A, Abidin ZZ. 2012. Batch adsorption of basic dye using acid treated kenaf fibre char: equilibrium, kinetic and thermodynamic studies. *J Chem Eng*, 181: 449-457.
- Misra DN. 1969. Adsorption on heterogeneous surfaces: A dubinin-radushkevich equation. *Surf Sci*, 18(2): 367-372.
- Mitrogiannis D, Markou G, Çelekli A, Bozkurt H. 2015. Biosorption of methylene blue onto *Arthrospira platensis* biomass: kinetic, equilibrium and thermodynamic studies. *J Environ Chem Eng*, 3(2): 670-680.
- Prats C, Francesch R, Arboix M, Pérez B. 2002. Determination of tylosin residues in different animal tissues by high performance liquid chromatography. *J Chromatogr B Analyt Technol Biomed Life Sci*, 766(1): 57-65.
- Rivera-Utrilla J, Sánchez-Polo M, Ferro-García MÁ, Prados-Joya G, Ocampo-Pérez R. 2013. Pharmaceuticals as emerging contaminants and their removal from water. A review. *Chemosphere*, 93(7): 1268-1287.
- Roginsky S, Zeldovich YB. 1934. The catalytic oxidation of carbon monoxide on manganese dioxide. *Acta Phys Chem USSR*, 1(554): 2019.
- Salazar-Rabago JJ, Leyva-Ramos R, Rivera-Utrilla J, Ocampo-Perez R, Cerino-Cordova FJ. 2017. Biosorption mechanism of Methylene Blue from aqueous solution onto White Pine (*Pinus durangensis*) sawdust: Effect of operating conditions. *Sustain Environ Res*, 27: 32-40.
- Sharma BM, Bečanová J, Scheringer M, Sharma A, Bharat GK, Whitehead PG, Klánová J, Nizzetto L. 2019. Health and ecological risk assessment of emerging contaminants (pharmaceuticals, personal care products, and artificial sweeteners) in surface and groundwater (drinking water) in the Ganges River Basin, India. *Sci Total Environ*, 646: 1459-1467.
- Topal M, Uslu G, Arslan Topal EI, Öbek E. 2013. Antibiyotiklerin tespiti ve arıtılması. *Erciyes Üniv Fen Bil Enst Fen Bil Derg*, 29(2): 185-199.
- Topp E, Renaud J, Sumarah M, Sabourin L. 2016. Reduced persistence of the macrolide antibiotics erythromycin, clarithromycin and azithromycin in agricultural soil following several years of exposure in the field. *Sci Total Environ*, 562: 136-144.
- Tunali Akar S, Ozdemir I, Sayin F, Akar T. 2021. Adsorption of diazo dye from aqueous solutions by magnetic montmorillonite composite. *CLEAN-Soil Air Water*, 49(2): 2000165.
- Wang G, Zhang Y, Wang S, Wang Y, Song H, Lv S, Li C. 2020. Adsorption performance and mechanism of antibiotics from aqueous solutions on porous boron nitride-carbon nanosheets. *Environ Sci Water Res Technol*, 6(6): 1568-1575.
- Weber WJ, Morris JC. 1963. Kinetics of adsorption on carbon from solution. *J Sanit Eng Div*, 89(2): 31-60.
- Yang S, Carlson KH. 2004. Solid-phase extraction-high-performance liquid chromatography-ion trap mass spectrometry for analysis of trace concentrations of macrolide antibiotics in natural and waste water matrices. *J Chromatogr A*, 1038(1-2): 141-155.
- Yang Z, Ren K, Guibal E, Jia S, Shen J, Zhang X, Yang W. 2016. Removal of trace nonylphenol from water in the coexistence of suspended inorganic particles and NOMs by using a cellulose-based flocculant. *Chemosphere*, 161: 482-490.
- Yin Y, Guo X, Yang C, Gao L, Hu Y. 2016. An efficient method for tylosin removal from an aqueous solution by goethite modified straw mass. *RSC advances*, 6(98): 95425-95434.
- Zafarani HR, Bahrololoom ME, Noubactep C, Tashkhourian J. 2015. Green walnut shell as a new material for removal of Cr (VI) ions from aqueous solutions. *Desalin Water Treat*, 55(2): 431-439.
- Zhang Y, Pan Z, Rong C, Shao Y, Wang Y, Yu K. 2019. Transformation of antibacterial agent roxithromycin in sodium hypochlorite disinfection process of different water matrices. *Sep Purif Technol*, 212: 528-535.